Observation of distorted Maxwell-Boltzmann distribution of epithermal ions in LHD

Observation of distorted Maxwell-Boltzmann distribution of epithermal ions in LHD

K. Ida,[1,2] T. Kobayashi,[1,2] M. Yoshinuma,[1,2] T. Akiyama,[1,2] T. Tokuzawa,[1] H. Tsuchiya,[1,2] K. Itoh,[3] and the LHD Experiment Group[1]

[1]*National Institute for Fusion Science, National Institutes of Natural Sciences, Toki, Gifu 509-5292, Japan*
[2]*SOKENDAI (The Graduate University for Advanced Studies), Toki, Gifu 509-5292, Japan*
[3]*Institute of Science and Technology Research, Chubu University, Kasugai 487-8501, Japan*

(Dated: November 17, 2017)

A distorted Maxwell-Boltzmann distribution of epithermal ions is observed associated with the collapse of energetic ions triggered by the tongue shaped deformation. The tongue shaped deformation is characterized by the plasma displacement localized in the toroidal, poloidal, and radial directions at the non-rational magnetic flux surface in toroidal plasma. Moment analysis of the ion velocity distribution measured with charge exchange spectroscopy is studied in order to investigate the impact of tongue event on ion distribution. A clear non-zero skewness (3rd moment) and kurtosis (4th moment -3) of ion velocity distribution in the epithermal region (within three times of thermal velocity) is observed after the tongue event. This observation indicates the clear evidence of the distortion of ion velocity distribution from Maxwell-Boltzmann distribution. This distortion from Maxwell-Boltzmann distribution is observed in one-third of plasma minor radius region near the plasma edge and disappears in the ion-ion collision time scale.

PACS numbers:

I. INTRODUCTION

The energetic particle driven MHD instabilities have been studied intensively in nuclear fusion research [1–4]. The understanding of the mechanism of this MHD instability and its impact on the bulk plasma are important in order to sustain the stable discharge with a significant amount of energetic particles in the plasma. It will be essential for the plasma in future devices such as ITER, where a significant amount of energetic alpha particles are produced. Various energetic particle driven MHD instabilities have been observed in heliotron plasmas [5, 6]. Associated with the energetic particle driven MHD bursts, the loss of energetic particles are also observed [7, 8]. The impact of the energetic particle driven MHD bursts on bulk plasmas has been also studied [9, 10]. However, there are few experimental results reported on the impact of these MHD instabilities on ion velocity distribution of bulk ions.

Recently a tongue-shaped deformation [11, 12] was observed just before the MHD bursts [10, 13]. The tongue-shaped deformation is characterized by a large displacement of equi-temperature surface localized in the toroidal, poloidal, and radial directions at the non-rational magnetic flux surface in the short time of ~ 100 μ sec. The tongue-shaped deformation appears in the relatively low density plasma with perpendicular neutral beam injection, where the significant amount of energetic trapped ions exist especially close to the neutral beam injection port. In this experiment, it was demonstrated that the tongue-shaped deformation triggers the loss of energetic particles and the distortion from Maxwell-Boltzmann distribution of carbon impurity ions. The distortion from Maxwell-Boltzmann distribution may cause the uncertainty in the evaluation of ion temperature and plasma flow velocity from carbon impurity using the charge exchange spectroscopy, where the Maxwell-Boltzmann distribution is assumed [10]. Therefore, quantitative evaluation of the distortion from Maxwell-Boltzmann distribution is necessary in order to understand the impact of energetic particle driven MHD bursts on bulk plasmas.

In this paper, the distortion of ions from Maxwell-Boltzmann distribution is quantitatively evaluated as a magnitude of skewness and kurtosis in space and time by using the moment analysis technique. The time period and region in the plasma where the distortion of ions from Maxwell-Boltzmann distribution appears are described. The distortion is associated with the loss of energetic ion indicated by the jump of intensity of the RF probe. The radial profiles of each moment of ion distribution and the change in radial electric field due to the energetic ion loss are presented and the impact of the distortion on the ion temperature and flow velocity measurements are discussed.

II. DISTORTION OF EPITHERMAL IONS FROM MAXWELL-BOLTZMANN DISTRIBUTION

The Large Helical Device (LHD) is a Heliotron-type device equipped with three tangential neutral beams with a beam energy of 160 - 180 keV and two perpendicular beams with a beam energy of 40 -50 keV. The charge exchange spectroscopy system has been installed in LHD to provide the radial profiles of ion temperature and toroidal rotation velocity of carbon impurity [14]. The charge exchange spectroscopy system used in this experiment gives

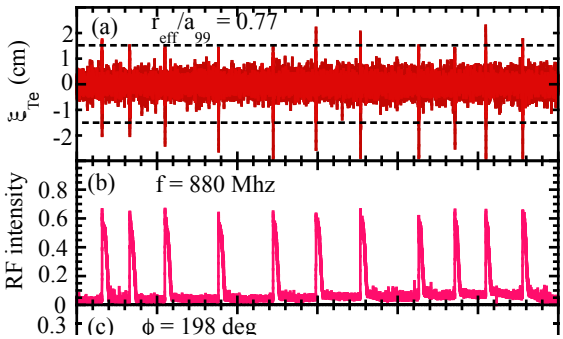

FIG. 1: Time evolution of (a) displacement of the plasma at $r_{\rm eff}/a_{99} = 0.77$, (b) RF intensity at 880 MHz measured with RF radiation probe, (c) magnetic field B_θ at toroidal angle of $\phi = 198°$, and (d) contour of spectra of charge exchange line of carbon impurity at $r_{\rm eff}/a_{99} = 0.79$.

the ion velocity distribution parallel to the magnetic field with a high time resolution of 0.8 ms and with spatial resolution of 36 channels from the magnetic axis ($R_{ax} = 3.6$ m) to plasma edge ($R = 4.6$ m). When the two perpendicular beams are injected into the plasma with relatively low density of 0.5 - 1.2 $\times$ 10^{19}m^{-3}, the MHD bursts appear associated with the enhancement of high frequency RF signals.

Figure 1 shows time evolutions of displacement of the plasma at $r_{\rm eff}/a_{99} = 0.77$, RF intensity at 880 MHz measured with RF radiation probe at ($\phi = 121°$), magnetic field B_θ at toroidal angle of $\phi = 198°$ and contour of spectra of charge exchange line of carbon impurity. Here the displacement of the plasma is calculated from the high frequency (1 - 10 kHz) change in temperature and quasi-state temperature gradient ($<$ 40 Hz) measured with ECE. The spikes of the displacement exceeding 2 cm at non-rational surface at $r_{\rm eff}/a_{99} = 0.77$ are the indication of tongue events [13]. The RF radiation probes are widely used as a timing indicator for the energetic ion loss from the plasma[15, 16], because RF probe has high time resolution and high sensitivity to the instability excited by the loss of energetic ions at the plasma edge [17, 18]. Associated with the tongue events, abrupt loss of energetic ions, MHD bursts and the red shift of the charge exchange line of carbon impurity are observed. Here,

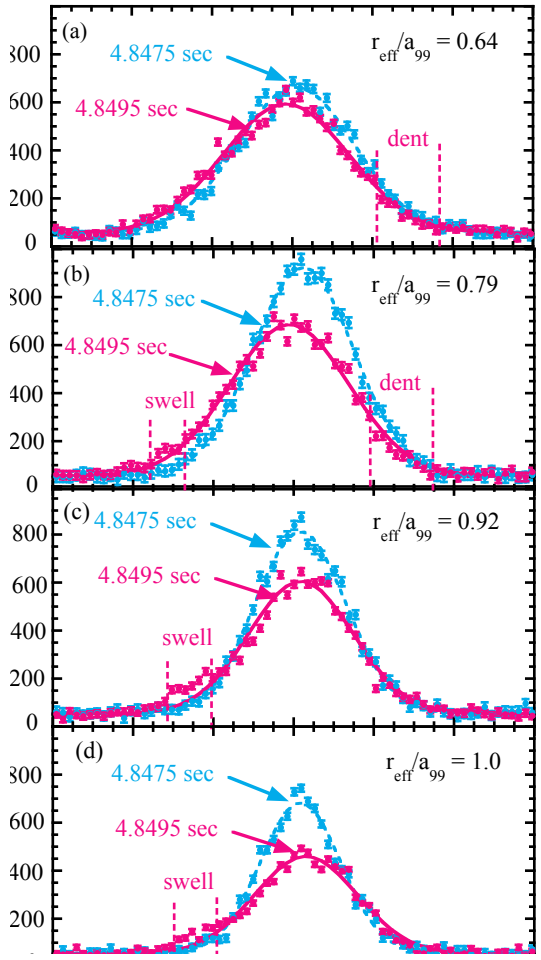

FIG. 2: Velocity distribution of carbon ions before ($t = 4.8475$ sec) and after ($t = 4.8495$ sec) the tongue event measured with charge exchange spectroscopy at (a) $r_{\rm eff}/a_{99} = 0.64$ ($R = 4.124$m), (b) $r_{\rm eff}/a_{99} = 0.79$ ($R = 4.261$m), (c) $r_{\rm eff}/a_{99} = 0.92$ ($R = 4.401$m), and (d) $r_{\rm eff}/a_{99} = 1.0$ ($R = 4.530$m).

the red shift corresponds to the negative velocity which is the flow velocity in the direction anti-parallel to the equivalent plasma current which produces the poloidal magnetic field (coubter-direction). In this discharge, two parallel NBIs and two perpendicular NBIs are injected into the plasma. The magnetic field is 2.7 T and the major, $R_{\rm ax}$ and effective minor radius $r_{\rm eff}$ are 3.6 m and 0.62 m, respectively. The plasma density is 0.55 $\times$ 10^{19} m^{-3} and the central electron and ion temperatures are 4 keV.

As seen in the velocity distribution of ions before and after the tongue events in figure 2, the decrease and increase of ion population are observed in the epithermal velocity range, which is one to two and one-half times of thermal velocity (1 - 2.5 V_{th}). Here the decrease is

called "dent," while the increase of population is called "swell." The "dent" appears in the positive velocity (co-traveling ions) and more significant in the plasma core at $r_{\rm eff}/a_{99} = 0.64$ and 0.79. In contrast, the "swell" appears in the negative velocity (counter-traveling ions) and more significant near the plasma edge at $r_{\rm eff}/a_{99} = 0.92$ and 1.0. The simultaneous change in the population of carbon ions both in co-traveling ($V > 0$) and counter-traveling ($V < 0$) particles are observed at $r_{\rm eff}/a_{99} = 0.79$.

Although the swell structures at $r_{\rm eff}/a_{99} = 0.92$ and 1.0 clearly exceed the noise level, the dent structures at $r_{\rm eff}/a_{99} = 0.64$ and 0.79 are close to the noise level in the spectra of one time slice. Therefore, further quantitative systematic analysis using conditioning averaged momentum analysis is necessary in order to identify the distortion of epithermal ions from the Maxwell-Boltzmann distribution.

III. MOMENT ANALYSIS TECHNIQUE

In order to evaluate the magnitude of this distortion quantitatively, the moment analysis is applied to the velocity distribution measured with charge exchange spectroscopy viewing the plasma toroidally. The 0th to the 4th moment of ion velocity distributions are defined as

$$M_0 = \int f(v)dv \tag{1}$$

$$M_1 = \frac{1}{M_0}\int v f(v)dv \tag{2}$$

$$M_2 = \frac{1}{M_0}\int (v-M_1)^2 f(v)dv \tag{3}$$

$$M_3 = \frac{1}{M_0 M_2^{3/2}}\int (v-M_1)^3 f(v)dv \tag{4}$$

$$M_4 = \frac{1}{M_0 M_2^2}\int (v-M_1)^4 f(v)dv. \tag{5}$$

When the velocity function $f(v)$ is Maxwell-Boltzmann distribution, each moment becomes $M_1 = V_s$, $M_2 = V_{th}^2/2$, $M_3 = 0$, $M_4 = 3$, where V_s and V_{th} are the projection of the flow velocity to the line-of-sight (mainly toroidal direction) and thermal velocity, respectively. Therefore, the finite values of skewness and M_3 and kurtosis ($M_4 - 3$) exceeding the noise level are clear evidence of distortion from Maxwell-Boltzmann distribution.

In order to improve the signal to noise ratio, the conditional averaging with respect to the time of RF sharp increase is applied for the series of MHD bursts ($\sim$ 30 events) in the time period ($\sim$ 1 sec) during which two

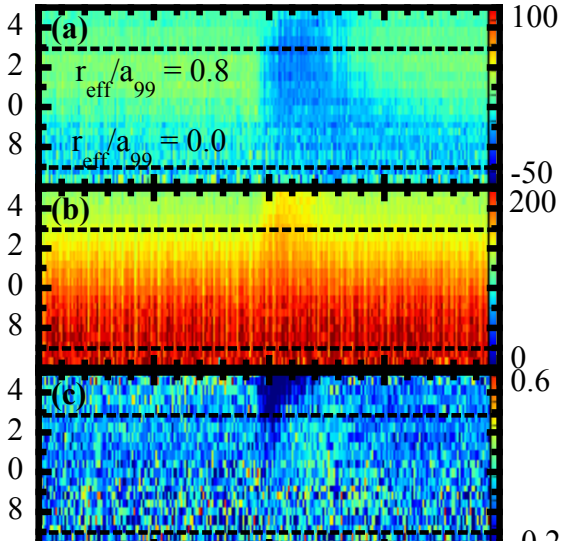

FIG. 3: Contour of (a) the 1st moment, (b) square root of the 2nd moment, (c) the 3rd moment, and (d) the 4th moment of ion velocity distribution of carbon at the tongue event.

tangential neutral beams and two perpendicular beams are injected into the plasma. Figure 3 shows the contour of each moment of ion velocity distribution in time at the collapse of energetic ions indicated by the sharp increase of the RF radiation probe signal at ($\phi = 121°$). Here τ is the relative time of the event with respect to the time of sharp increase of the RF radiation probe signal. The major radius of magnetic axis and plasma edge are 3.7m and 4.5m, respectively. The changes in 1st and 2nd moments of ion velocity distribution start at $R = 4.2$m, where the large displacement of the plasma is observed, and fast propagation inward and outward are also observed. The decrease of 1st moment of ion velocity distribution are observed in the wide region plasma ($R > 3.9$ m) with 3 - 5 ms after the sharp increase of RF intensity. The sharp increases of 2nd moment of ion velocity distribution are observed at each burst and the sharp increases are more visible near the plasma edge. This change in ion velocity distribution also gives an apparent increase of thermal velocity.

The change in 3rd and 4th moments of ion velocity distribution are not so clear compared with the change in 1st and 2nd moments of ion velocity distribution. The sudden decrease of 3rd moment of ion velocity distribu-

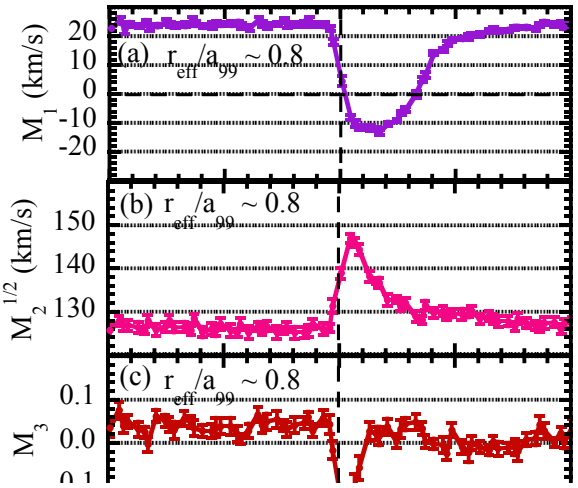

FIG. 4: Time evolution of (a) 1st moment (M_1), (b) square root of 2nd moment (M_2), (c) 3rd moment (M_3), and (d) 4th moment (M_4) - 3 of ion velocity distribution of carbon at $r_{\rm eff}/a_{99} = 0.8$, at the tongue event. Here τ is the relative time of the event respect to the time of the sharp increase of RF intensity.

tion is observed near the plasma edge ($R > 4.2$m) and the time period of the decrease is 1 - 3 ms. This decrease indicates that the ion distribution is distorted from Maxwell-Boltzmann distribution. The magnitude of the distortion increases toward the plasma edge and the duration of the distortion is 1 - 3 ms and becomes longer near the plasma edge. There is a minute decrease in magnitude and time of the 4th moment of ion velocity distribution, although the decrease is not clear in the contour plot.

Figure 4 shows the time evolution of each moment with the average in space (3 data points) and time (8 data points) at $r_{\rm eff}/a_{99} \sim 0.8$, where the large displacement of the plasma appears as the tongue deformation event. The error bars indicated in figure 4 (a)-(d) and figure 5 (a)-(d) are defined as $\sigma/\sqrt{N}$, where σ is a standard deviation of N data points averaged and $N = 24$ (3×8). The 1st moment of ion velocity distribution is 25 km/s, which corresponds to the toroidal rotation velocity in co-direction. After the tongue event, the 1st moment decreases by 35 km/s and becomes negative (-10 km/s) within 1 ms. This is due to the simultaneous decrease of co-traveling particles and increase of counter-traveling particles. The square root of the 2nd moment of ion velocity distribution is 127 km/s, which corresponds to the thermal velocity of 180 km/s. The change in the 1st moment of ion velocity distribution is 20 % of thermal velocity. The 3rd moment of ion velocity distribution shows the sharp decrease after the tongue event and M_3 falls below -0.1. However, it returns to zero within 2 ms, which is much shorter than the recovery time of the 1st moment of ion velocity distribution. The signal to noise ratio is improved especially for the 4th moment and (M_4-3) falls below -0.2 after the tongue event, and returns to zero within 2 ms, which is also shorter than the recovery time of square root of the 2nd moment of ion velocity distribution. These data show that the change of the 1st moment and the 2nd moment of ion distribution (apparent velocity and apparent ion temperature) is due to the relaxation of the distortion from Maxwell-Boltzmann distribution, which is identified by the sharp and short decrease of M_3 and M_4-3.

IV. PROFILES OF EACH MOMENT AND RADIAL ELECTRIC FIELD

Figure 5 shows the radial profiles of each moment with the average in space (3 data points) and time (8 data points) 0.4 ms before and 0.6 ms after the tongue deformation event. The radial profiles of the radial electric field before and after the tongue event are also plotted. The distortion from Maxwell-Boltzmann distribution is observed in the outer half of the plasma minor radius of $r_{\rm eff}/a_{99} > 0.6$ as indicated by the decrease of the 3rd and the 4th moments of ion velocity distributions. The distortion magnitude increases as the minor radius is increased and becomes maximum at the plasma edge of ($r_{\rm eff}/a_{99} = 1$). Although the value of the square-root of the 2nd moment (which is equivalent to thermal velocity of ion in Maxwell-Boltzmann) increases after the collapse, its radial gradient even decreases in the whole plasma region inside LCFS. The increase of the 2nd moment of ion distribution is due to the thermalization of the non-Maxwell-Boltzmann distribution of ions. It is interesting that the change in the 1st and the 2nd moments due to this collapse event extends to the plasma center, while the distortion from Maxwell-Boltzmann distribution is only outer region of the plasma. The distortion from Maxwell-Boltzmann distribution is localized in time and space, but the effect (change in the 1st and the 2nd moments) extends longer in time and becomes wider in space due to the thermalization of ions with non-Maxwell distribution.

As seen in figure 5, both the 3rd and 4th moments (M_3 and M_4-3) become zero 2.7 ms after the collapse, which indicates that the ion distribution becomes Maxwell-Boltzmann distribution by the thermalization. However, the radial profiles of 1st and 2nd moment at 2.7 ms differ from that before the collapse (-0.4ms). This result

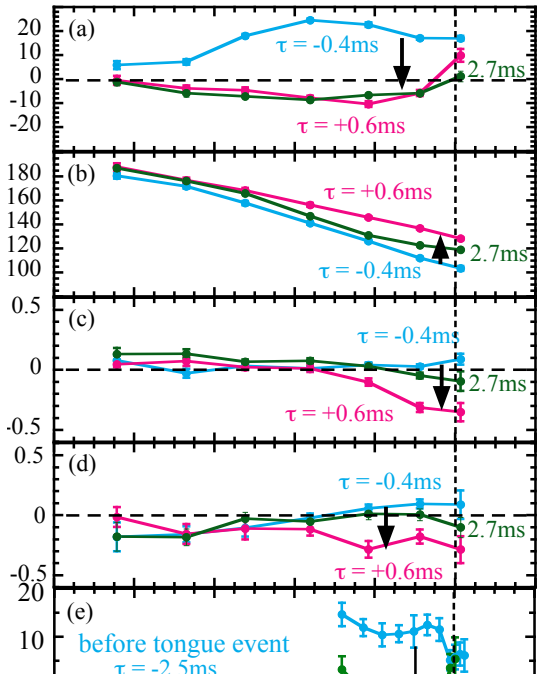

FIG. 5: Radial profile of (a) 1st moment (M_1), (b) square root of 2nd moment (M_2), (c) 3rd moment (M_3), (d) 4th moment (M_4) - 3 of ion velocity distribution of carbon 0.4ms before and 0.6ms and 2.7ms after the collapse, and (e) radial electric field 2.5ms before and 2.5ms after the tongue event.

shows the decrease in toroidal rotation velocity and increase of ion thermal velocity (ion temperature) observed at $t = 2.7$ ms is due to the thermalization of the distorted Maxwell-Boltzmann distribution at $t = 0.6$ ms. At $t = 2.7$ ms, the increase of the ion thermal velocity at $r_{\rm eff}/a_{99} = 0.8$ disappears, and the increase of the edge ion thermal velocity at $r_{\rm eff}/a_{99} = 1$ remains. The gradient of thermal velocity near the edge ($r_{\rm eff}/a_{99} = 0.8 - 1.0$), where the negative radial electric field appears, becomes smaller after the collapse of energetic ions. It is also interesting that the shift of mean flow velocity (toroidal flow velocity) is almost unchanged in the short time period of 2.7 ms after the collapse.

The radial profiles of the radial electric field are measured with charge exchange spectroscopy before and after the tongue event in the region where the distortion from the Maxwell-Boltzmann distribution is observed. After the tongue event, this positive radial electric field decreases and even changes its sign to negative due to the loss of energetic ions from the perpendicular NBI. The change in the radial electric field from positive to nearly zero near the plasma edge is consistent with the radial electric field inferred from the perpendicular velocity measured with doppler reflectometor [13] and heavy ion beam probe (HIBP) measurements [10].

The orbit of trapped ion is sensitive to the radial electric field and the positive radial electric field prevents the orbit loss of trapped ion in helical plasmas. The disappearance of the positive radial electric field is a strong candidate for causing the loss of epithermal trapped carbon ions measured with charge exchange spectroscopy. The change in radial electric field and poloidal rotation velocity is localized near the plasma edge and has a maximum value at $r_{\rm eff}/a_{99} > 0.9$, while the change in the 1st moment (which is equivalent to toroidal rotation velocity of ion in Maxwell-Boltzmann) is wider and has a maximum value at $r_{\rm eff}/a_{99} > 0.7$.

It should be noted that the ion species in which the distortion from Maxwell-Boltzmann distribution is observed is carbon impurity and not the bulk ion during the slowing down process of energetic particles from NBI. In order to investigate the mechanism causing the tongue-shaped deformation, which triggers the loss of energetic ions, it is necessary to measure the velocity distribution of bulk ions. The distortion from Maxwell-Boltzmann distribution of carbon impurity is speculated to be the result of flattening or of decrease of the gradient of epithermal trapped ions associated with the rapid change in the radial electric field due to the loss of energetic bulk ions. The detailed mechanism that causes the distortion from Maxwell-Boltzmann distribution of carbon impurity is discussed in the next section.

V. DISCUSSION AND SUMMARY

The parameter regime in which the distorted Maxwell-Boltzmann distribution of epithermal ions is observed and the possible mechanism causing this distortion are discussed in this section. This distortion is observed only in the low density ($< 1.2 \times 10^{19}$m^{-3}) with two perpendicular NBIs. No distortion is observed in the plasma with one perpendicular NBI. The changes in the 3rd moment (-ΔM_3) and the 4th moment (-ΔM_4) of ion velocity distribution are significantly large at the low density of 0.5×10^{19}m^{-3} and decrease as the electron density is increased as seen in figure 6. Here ΔM_3 and ΔM_4 are given as $\Delta M_3 = M_3(t{=}{+}0.6\text{ms}) - M_3(t{=}{-}0.4\text{ms})$ and $\Delta M_4 = M_4(t{=}{+}0.6\text{ms}) - M_4(t{=}{-}0.4\text{ms})$, respectively. At the line averaged electron density of 1×10^{19}m^{-3}, the changes in 3rd and 4th moments are still present but are relatively small (≤ 0.1). The magnitude of the change in the 3rd and 4th moments is less sensitive to the number of parallel NBIs, which implies that the mechanism causing the distorted Maxwell-Boltzmann can be attributed to the trapped ions with banana orbit rather than the passing ions of the NBI.

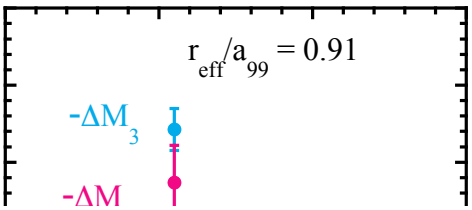

FIG. 6: The change in 3rd moment (-ΔM_3) and 4th moment (-ΔM_4) of ion velocity distribution of carbon during the collapse as a function of line averaged density.

The center of the banana orbit of co-traveling particle is located on the inner side of the line of sight. On the other hand, the center of the banana orbit of counter-traveling particle is located one the outer side of the line of sight. Therefore, the decrease of trapped particle gradient results in a simultaneous decrease of co-traveling particles and an increase of the counter-traveling particles, and the decrease of 1st moment. The flattening of trapped ion gives the decrease of the 1st moment of ion distribution and an apparent increase of plasma flow velocity in the counter-direction.

The tongue deformation triggers the collapse of energetic ions detected by the sharp increase of RF intensity and the abrupt change in radial electric field and poloidal rotation velocity measured with charge exchange spectroscopy. The radial electric field is positive before the collapse of energetic ions and the MHD burst (stationary m/n=1/1 mode and tongue deformation phases), but it changes its sign to negative. The finite skewness and kurtosis are observed in the outer half of the plasma only within 1 - 2 ms after the collapse of energetic ions indicated by the sharp increase of RF intensity. The distortion of ion from Maxwell-Boltzmann distribution disappears due to the thermalization process in the collision time scale between bulk ion and carbon impurity ions of $\sim$ 1 ms. Therefore, the measurements of ion temperature and flow velocity are not affected by the distortion from Maxwell-Boltzmann distribution 2 ms after the RF intensity sharp increase. After this thermalization process, the decreases of thermal velocity (and ion temperature) gradient and toroidal flow shear are observed as an impact of tongue event on bulk plasma parameters.

There are similarities between the tongue deformation and the solitary perturbations (SPs) observed in the KSTAR tokamak [19–21]. Solitary perturbations (SPs) localized both poloidally and radially are detected within $\sim$100 μs before the partial collapse of the high pressure gradient boundary region (called pedestal). Both perturbations have no mode structure and are poloidally, toroidally, and radially localized and appear $\sim$100 μs before the collapse (ELM or MHD burst). This crash onset is detected by the RF probe, which is sensitive to the instability due to the energetic ion loss at the plasma boundary. Between the collapses a quasi-stable mode (quasi-stable edge-localized mode QSM or stationary 1/1 mode) with mode structure appears. These quasi-stable modes (QSM or stationary 1/1 mode) do not directly trigger the collapse.

The authors would like to thank the technical staff of LHD for their support of these experiments. The authors also would like to thank Dr. G.S. Yun of POSTECH for the RF probe collaboration and useful discussions. This work is partly supported by JSPS KAKENHI Grant Numbers JP16K13923, JP15H02336, JP16H02442. This work is also partly supported by the National Institute for Fusion Science grant administrative budget NIFS10ULHH021.

[1] C.Z. Cheng and M.S. Chance, *Phys. Fluids* **29**, 3695 (1986).
[2] L. Chen, *Phys. Plasmas* **1**, 1519 (1994).
[3] K.L.Wong, *Plasma Phys. Control. Fusion.* **41**, R1 (1999).
[4] W.W. Heidbrink, *Phys. Plasmas* **15**, 055501 (2008).
[5] K. Toi, M. Takechia, M. Isobe, N. Nakajima, M. Osakabe, S. Takagia, T. Kondob, G. Matsunagaa, K. Ohkunia, M. Sasao, S. Yamamotoa, S. Ohdachi, S. Sakakibara, H. Yamada, K.Y. Watanabe, D.S. Darrowc, A. Fujisawa, M. Goto, K. Ida, H. Idei, H. Iguchi, S. Leed, S. Kado, S. Kubo, O. Kaneko, K. Kawahata, K. Matsuoka, T. Minami, S. Morita, O. Motojima, K. Narihara, S. Nishimura, N. Ohyabu, Y. Oka, S. Okamura, T. Ozaki, K. Sato, M. Sato, A. Shimizua, T. Shimozuma, Y. Takeiri, K. Tanaka, T. Tokuzawa, K. Tsumori, I. Yamada, Y. Yoshimura and CHS and LHD Experimental Groups, *Nucl. Fusion* **40**, 1349 (2000).
[6] S. Yamamoto, K. Toi, S. Ohdachi, N. Nakajima, S. Sakakibara, C. Nührenberg, K.Y. Watanabe, S. Murakami, M. Osakabe, M. Goto, K. Kawahata, S. Masuzaki, S. Morita, K. Narihara, Y. Narushima, N. Ohyabu, Y. Takeiri, K. Tanaka, T. Tokuzawa, H. Yamada, I. Yamada, K. Yamazaki and LHD Experimental group, *Nucl. Fusion* **45**, 326 - 336 (2005).

[7] K. Nagaoka, M. Isobe, K. Toi, A. Shimizu, A. Fujisawa, S. Ohshima, H. Nakano, M. Osakabe, Y. Todo, T. Akiyama, Y. Nagashima, C. Suzuki, S. Nishimura, Y. Yoshimura, K. Matsuoka, and S. Okamura, *Phys. Rev. Lett.* **100**, 065005 (2008).

[8] K. Ogawa, M. Isobe, K. Toi, F. Watanabe, D.A. Spong, A. Shimizu, M. Osakabe, S. Ohdachi, S. Sakakibara, and LHD Experiment Group, *Nucl. Fusion* **50**, 084005 (2010).

[9] S. Ohshima, S. Kobayashi, S. Yamamoto, K. Nagasaki, T. Mizuuchi, H. Okada, T. Minami, K. Hashimoto, N. Shi, L. Zang, K. Kasajima, N. Kenmochi, Y. Ohtani, Y. Nagae, K. Mukai, H.Y. Lee, H. Matsuura, M. Takeuchi, S. Konoshima and F. Sano, *Nucl. Fusion* **56**, 016009 (2016).

[10] X.D. Du, K. Toi, S. Ohdachi, M. Osakabe, T. Ido, K. Tanaka, M. Yokoyama, M. Yoshinuma, K. Ogawa, K.Y. Watanabe, T. Akiyama, M. Isobe, K. Nagaoka, T. Ozaki, S. Sakakibara, R. Seki, A. Shimizu, Y. Suzuki, H. Tsuchiya and the LHD Experiment Group, *Nucl. Fusion* **56**, 016002 (2016).

[11] L.A. Arstimovich, A Physicist's ABC on Plasma, First edition 1978, Revised from the 1976 Russian Edition, English translation, Mir Publishers, (Moscow, 1978).

[12] K. Itoh, S.-I. Itoh, K. Ida, and Y. Kosuga, *J. Phys. Soc. Jpn.* **85**, 094504 (2016).

[13] K. Ida, T. Kobayashi, K. Itoh, M. Yoshinuma, T. Tokuzawa, T. Akiyama, C. Moon, H. Tsuchiya, S. Inagaki, and S.-I. Itoh, *Sci. Rep.* **6**, 36217 (2016).

[14] M. Yoshinuma, K. Ida, M. Yokoyama, M. Osakabe, K. Nagaoka, S. Morita, M. Goto, N. Tamura, C. Suzuki, S. Yoshimura, H. Funaba, Y. Takeiri, K. Ikeda, K. Tsumori, O. Kaneko, and LHD Experiment Group, *Fusion Sci. Technol.* **58**, 375 (2010).

[15] W. W. Heidbrink, M. E. Austin, R. K. Fisher, M. García-Muñoz, G. Matsunaga, G. R. McKee, R. A. Moyer, C. M. Muscatello, M. Okabayashi, D. C. Pace, K. Shinohara, W. M. Solomon, E. J. Strait, M. A. Van Zeeland and Y. B. Zhu, *Plasma Phys. Control. Fusion.* **53**, 085028 (2011).

[16] K. Saito, R. Kumazawa, T. Seki, H. Kasahara, G. Nomura, F. Shimpo, H. Igami, M. Isobe, K. Ogawa, K. Toi, M. Osakabe, M. Nishiura, T. Watanabe, S. Yamamoto, M. Ichimura, T. Mutoh and LHD Experiment Group, *Plasma Sci. Technol.* **15**, 209 (2013).

[17] P. Schild, G.A. Cottrell, and R.O. Dendy, *Nucl. Fusion* **29**, 834 (1989).

[18] R. O. Dendy, K. G. McClements, and C. N. Lashmore-Davies, *Phys. Plasmas* **1**, 1918 (1994).

[19] G. S. Yun, W. Lee, M. J. Choi, J. Lee, H. K. Park, B. Tobias, C. W. Domier, N. C. Luhmann, Jr., A. J. H. Donné, and J. H. Lee, *Phys. Rev. Lett.* **107**, 045004 (2011).

[20] G. S. Yun, W. Lee1, M. J. Choi, J. Lee, H. K. Park, C. W. Domier, N. C. Luhmann Jr., B. Tobias, A. J. H. Donné,, J. H. Lee, Y. M. Jeon, S. W. Yoon, and KSTAR team *Phys. Plasmas* **19**, 056114 (2012).

[21] J. E. Lee, G. S. Yun, W. Lee, M. H. Kim, M. Choi, J. Lee, M. Kim, H. K. Park, J. G. Bak, W. H. Ko & Y. S. Park, *Sci. Rep.* **7**, 45075 (2017).